

## Measurement of Stress Birefringence Patterns in Molten Polymers Flowing through Geometrically Complex Channels

CHANG DAE HAN, *Department of Chemical Engineering, Polytechnic Institute of New York, Brooklyn, New York 11201*

### Synopsis

Measurements were taken of stress birefringence patterns in molten polymers flowing through geometrically complex channels. Six different flow channels were constructed for experiment, some representing the flow geometries of spinnerettes encountered in fiber spinning, and others representing mold cavities encountered in injection molding. All the flow channels had two glass windows, which permitted one to take photographs of the flow birefringence patterns of molten polymers with the aid of a polariscope. Quantitative information on the stress distributions in a flow channel was obtained, with the aid of the stress-optical laws, from the pictures taken of both isochromatic and isoclinic fringe patterns. The significance of flow birefringence measurement is discussed from the standpoint of die design for extrusion operation and mold design for injection molding operation.

### INTRODUCTION

In some polymer operations, such as in fiber spinning, injection molding, and blown film extrusion, molten polymers often have to flow through a geometrically complex channel. From the processing point of view, it is of practical interest to correlate the rheological behavior of polymeric materials in a given flow field to processing variables affecting pressure drops, for instance, and the mechanical properties of finished products. Unfortunately, however, a rigorous theoretical analysis of the flow problems, for instance, to predict stress distributions in a complicated flow field, is very difficult to carry out, if not impossible.

It is a well-accepted fact today that many polymer melts exhibit viscoelastic behavior under processing conditions of industrial interest. On the other hand, the extent of viscoelastic behavior of a polymer melt depends in some measure on the flow geometry of the die, which affects the extent of deformation and the deformation history. It is believed today that the elastic property, rather than the viscous property, is primarily responsible for the excessively large pressure drop experienced at the die entry in the extrusion operation, and for the residual stress ("frozen-in" stress) present in an injection molded article.

Whereas a strictly theoretical approach may not be attractive to fully understand the rheological behavior of viscoelastic fluids in a complex flow channel, some experimental approach may be very useful. One experimental

approach which has been proven useful is the flow birefringence technique. In recent years, several researchers<sup>1-6</sup> have applied the flow birefringence technique to studying the rheological behavior of polymer solutions and melts in both the entrance region and the exit region. As one may surmise, there are numerous instances in the polymer processing industry where flow channels have a geometry far more complicated than a straight channel or a converging channel.

Very recently, the author has carried out an experimental study on the flow birefringence of molten polymers flowing through geometrically complex flow channels. Several flow channels were constructed for the study; some were aimed at simulating spinnerettes of complex nature; and others simulating mold cavities with and without a metal insert. In the present paper, we shall present some representative results of the study and discuss the significance of the results from the standpoint of polymer operations.

## EXPERIMENTAL

The apparatus consisted of three major parts: (a) the polymer melt feed system, (b) the test channel (die), and (c) the optical system, as schematically shown in Figure 1.

### Polymer Feed System

The polymer melt feed system consisted of a 1-in.-diameter Killion extruder and a length of stainless steel tubing (0.5 in. I.D. and about 2 ft long). This rather long tubing was used to calm down the helical motion of the melt created by the screw in the extruder before the melt actually reaches the die inlet.

### Die Design

Basically, two sets of dies were constructed for the present study. One set of three dies is shown schematically in Figure 2. Die 2a represents a spinnerette hole with two tapered sections in series; die 2b represents a spinnerette hole with no land length; die 2c represents a rectangular mold cavity with a sprue in the front.

Another set of three dies is shown schematically in Figure 3. These dies simulate mold cavities with a "metal insert." In recent years, the injection molding industry has shown a steadily growing interest in producing molded articles with a metal insert (e.g., electric sockets, automobile steering wheels). The primary purpose of using the dies shown in Figure 3 was to better understand the stress distributions at various locations in the flow field. In the dies shown in Figure 3, the metal insert was suspended at the center so that the melt feed stream split into two separate streams at the entrance of the die and left the flow channel as separate streams.

In order to observe the flow birefringent patterns, glass windows were placed on either side of the die over the entire flow field. The glass was a strain-free Vycor glass manufactured by the Corning Glass Company. The pieces were ground, cut, and polished by the Dell Optics Company. All metal

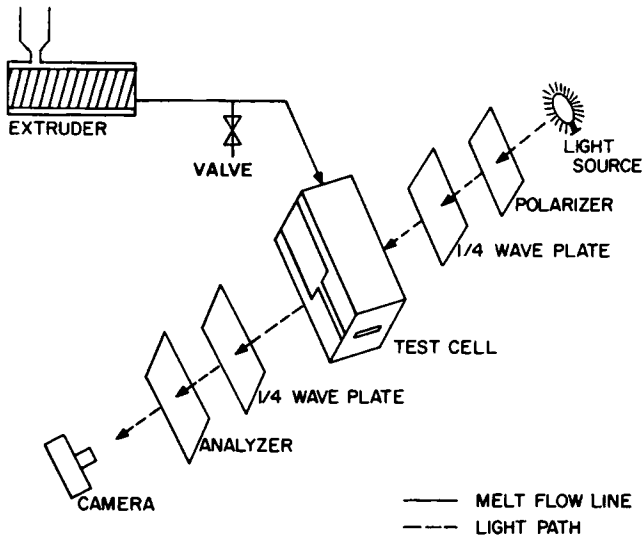


Fig. 1. Schematic diagram of apparatus.

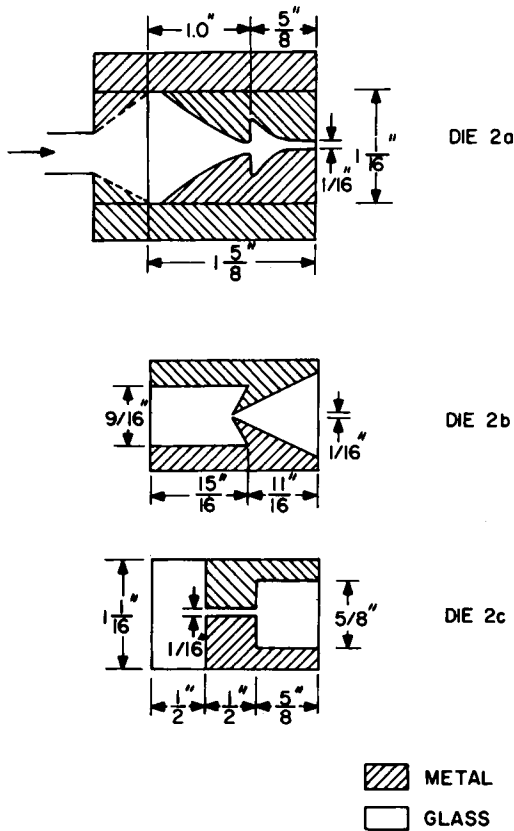


Fig. 2. Schematic diagram of flow channels tested.

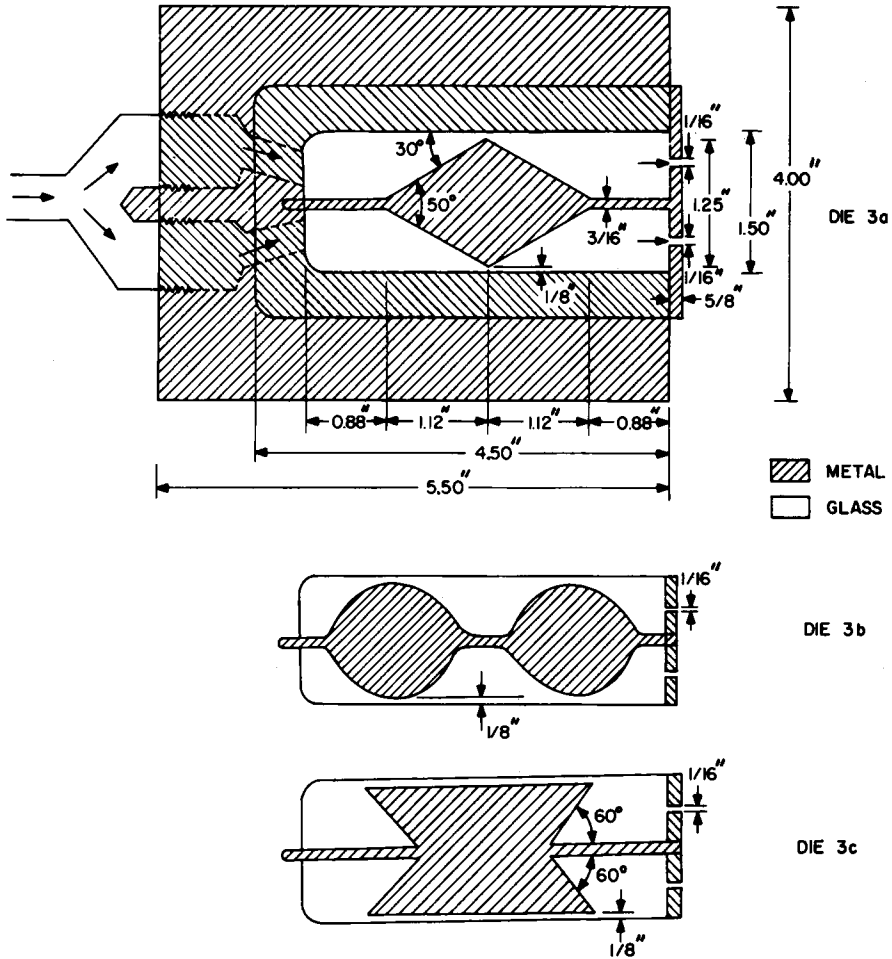


Fig. 3. Schematic diagram of flow channels with metal insert.

surfaces of the die were covered with custom-made band and strip mica-insulated electric heaters; and in order to minimize heat losses to the surroundings, a thick layer of asbestos was placed over all the heating surfaces.

### Optical System

The optical system used is the same as that described in our earlier paper.<sup>5</sup> Basically, it consists of a light source, interference filter, diffusion screen, polarizer, quarter wave plates, analyzer, and a camera (see Fig. 1). Both white light and monochromatic light sources were used in the study. The white light source was used to obtain colored isochromatic fringe patterns and to easily identify the isoclinic fringes.

### Experimental Procedure

The experimental procedure used is essentially the same as that described in our earlier paper.<sup>5</sup> Briefly stated, isochromatic fringes were recorded by

using circularly polarized light (i.e., with the quarter-wave plates in place), and isoclinic patterns were recorded by first removing the quarter-wave plates from the light path and then rotating the polarizer and the analyzer together, keeping them crossed all the time. Photographs were taken of isoclinic patterns at orientation angles of 10, 20, 30, 40, 50, 60, 70, 80, and 90 degrees.

### Materials

The materials used for experiment were polystyrene (Dow Chemical, STY-RON 686), and high-density polyethylene (Union Carbide, DMDJ 4309). These polymers were used mainly because the stress optical coefficients of the materials had already been determined in our earlier study.<sup>5</sup>

## RESULTS AND DISCUSSION

### Stress Birefringence Patterns and Their Rheological Implication

When polarized light enters an optically anisotropic medium, the beam separates into two plane-polarized components in the direction of the principal stresses. When the two components emerge from the medium, they have a certain relative retardation. Furthermore, under certain conditions extinction of the emerging beam of light occurs, giving rise, when the entire field is viewed, to isoclinic fringe patterns when  $2\theta = N\pi$  and to isochromatic fringe patterns when  $\alpha/2 = N\pi$ . Here,  $\theta$  denotes the direction of the principal stresses,  $\alpha$  is the angular phase difference (or retardation) of the emerging beam of light, and  $N$  is an integer. Isochromatics appear as a pattern of light and black bands when monochromatic light is used, and as bands of the same color when white light is used. Each band corresponds to a constant value of the maximum shearing stress. Isoclinics appear as other dark regions when the maximum shearing stress makes a certain angle ( $2\theta = N\pi$ ) with the axis of polarization of the incident light. These isoclinics appear only when plane-polarized light is employed, whereas the isochromatics appear whether the incident light is plane or circularly polarized.

Representative pictures of isochromatic fringe patterns are given in Figure 4 for melt flow in die 2a, in Figure 5 for melt flow in die 2b, and in Figure 6 for melt flow in die 2c. Figures 4, 5, and 6 each present four pictures labeled (a), (b), (c), and (d), in which flow rate increases in alphabetical order. It can be seen that, as the flow rate is increased, the number of fringes increases accordingly. Since each band (black and white) corresponds to the locus of points with a constant principal stress difference and also the locus of points of maximum shear stress, one can make some important observations from these figures.

It is seen in Figure 4a that the fringes tend to emanate from points on the die wall having the greatest curvature and develop toward the centerline of the die along the direction of flow. This is true for both parts of the die. As the flow rate is increased (i.e., as one moves from Figure 4a to Figure 4d), the two fringes emanating from the walls meet at the center, combine with each other, and then move simultaneously in different directions. It should be

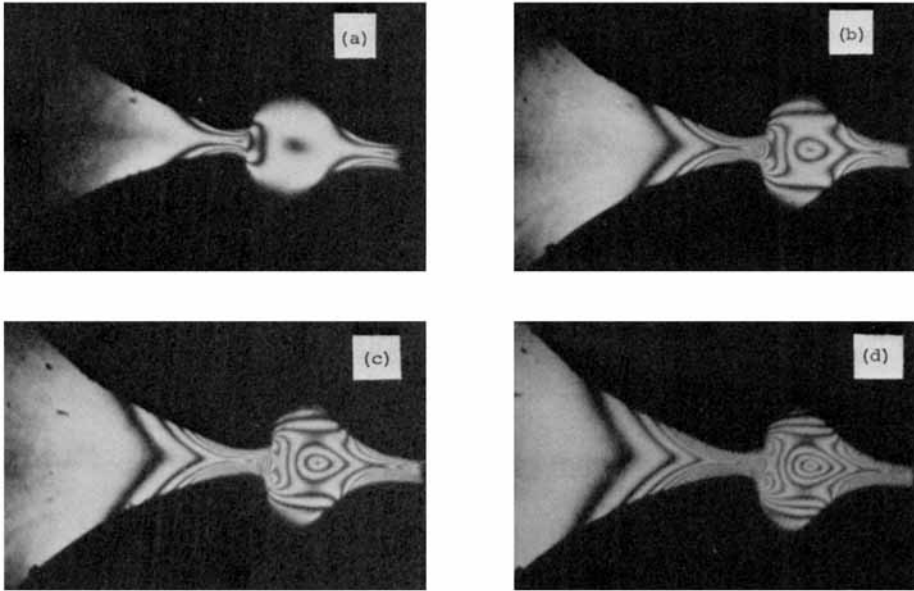


Fig. 4. Isochromatic fringe patterns in die 2a for polystyrene at 200°C: (a)  $Q = 0.78$  cc/min; (b)  $Q = 2.85$  cc/min; (c)  $Q = 5.15$  cc/min; (d)  $Q = 7.22$  cc/min.

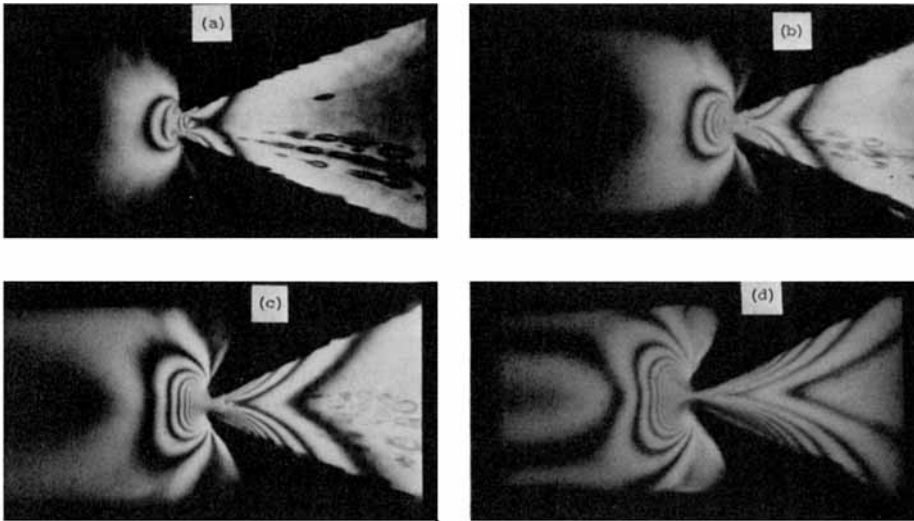


Fig. 5. Isochromatic fringe patterns in die 2b for polystyrene at 200°C: (a)  $Q = 0.81$  cc/min; (b)  $Q = 3.54$  cc/min; (c)  $Q = 7.21$  cc/min; (d)  $Q = 9.23$  cc/min.

noted that the stress concentration is highest at the location where most fringes are. On the basis of this fact, one can conclude from Figure 4 that as a melt flows from the left to the right, the highest stress concentration occurs at the corner of the left half of the die, and that stresses relax in the chamber of the right half of the die. Then, stresses start to build up again as the polymer melt flows toward the die exit.

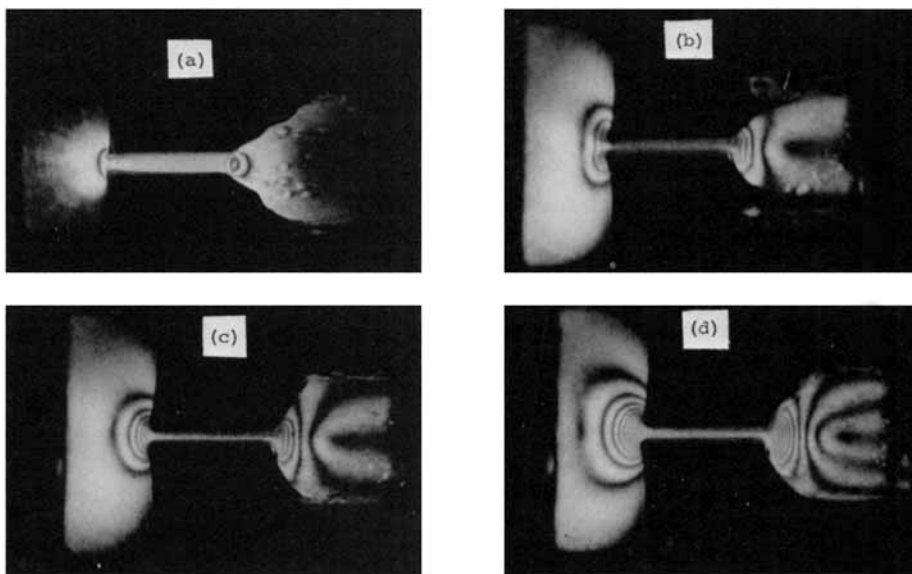


Fig. 6. Isochromatic fringe patterns in die 2c for polystyrene at 200°C: (a)  $Q = 1.21$  cc/min; (b)  $Q = 3.13$  cc/min; (c)  $Q = 6.54$  cc/min; (d)  $Q = 8.91$  cc/min.

Now, one may wish to know what is the commercial value of a die design, such as die 2a, having two converging sections in series. In recent years, the fiber industry has been interested in producing fibers of high tenacity. For a given fiber-forming material, the geometry of spinnerette holes has been proven to be a very important factor which can significantly improve the mechanical/physical properties of the finished fiber. In general, it appears that greater orientation of macromolecules within a spinnerette hole would improve the tenacity of the spun fiber, provided that the molecular orientation achieved within the spinnerette holes is retained in the finished fiber. Along this line of thought, one would like to know which geometry of many possible spinnerette hole shapes might give rise to the greatest molecular orientation.

In recent years, much has been discussed in the literature about the entrance region flow of viscoelastic fluids. Some have reported flow patterns in the entrance region<sup>7,8</sup>; others have determined velocity distributions experimentally<sup>9,10</sup>; and still others have determined stress distributions experimentally.<sup>1,5</sup> All these studies indicate, either directly or indirectly, that considerable molecular orientation can be achieved as a fluid enters into a small opening from a large reservoir upstream. The molecular orientation achieved in the entrance region is attributed to the existence of the accelerative flow field, sometimes referred to as the converging flow field or extensional flow field. Some earlier studies of stress measurements by Han and Drexler<sup>5</sup> indicate also that the amount of stresses that can be built up in the melt at the entrance region depends on the entrance geometry of the die, and that stresses initially present in the melt at the entrance region subsequently relax to a certain degree as the fluid flows through a long straight section of the die. A recent study by Han<sup>11</sup> demonstrates that when there is no straight section of a die (i.e., a die having a converging section only), stresses keep increasing as the fluid approaches the die exit.

Die 2b represents a spinnerette hole of zero die length, with an entrance angle of  $240^\circ$ . One might think that an entrance angle greater than  $180^\circ$  is rather uncommon in spinning operations. In most cases, the entrance angle is kept somewhat between  $60^\circ$  to  $120^\circ$ , depending on the material to be spun, although there is no clear-cut theory suggesting a relationship between the entrance angle and the rheological properties of a fiber-forming material.

It is interesting to note that, in commercial spinning operations, the fiber-forming materials being transported from the polymerization reactors invariably contain impurities, which can either partially block spinnerette holes or cause breakage of spinning lines. Hence, cleaning the spinnerettes is a major problem which interrupts the continuous operation of spinning machines. Therefore, it is highly desirable either to eliminate the impurities from the fiber-forming materials before they actually reach the spinning machine or collect the impurities somewhere in the spinning system. Details of how one does this in practice is a carefully guarded secret in the fiber industry.

Figure 6 gives isochromatic fringe patterns in polystyrene melts which flow into a small, straight die section from a large reservoir, and into a large area from a small die section. This geometry was chosen to simulate the flow field in a rectangular mold of a type which may be found in some injection molding operations. For instance, one may consider the small straight section, which connects the two rectangular sections, as a sprue in the injection molding operation. There are some similarities in the isochromatic fringe patterns of the converging flow field on the left half of the die and the diverging flow field on the right half of the die, although a detailed study will reveal some subtle, important differences between the two. Note that the isochromatic fringe patterns in the straight die section connecting the two rectangular sections are not clearly distinguishable. This is due to the fact that the fringes in this area are clustered too closely together. The pattern would be parallel to the die wall in the region far from the entrance and exit regions. Such a fringe pattern in the fully developed region is reported in an earlier paper by Han and Drexler.<sup>5</sup>

As mentioned above, at a fixed flow rate (i.e., for one photograph of isochromatics), we have taken photographs of isoclinis at orientation angles of from  $0^\circ$  to  $90^\circ$  in increments of  $10^\circ$ . Figure 7 displays representative photographs of isoclinic fringe patterns, one for each die, at an orientation angle of  $90^\circ$ . Space limitations here do not permit us to present photographs taken at other orientation angles. It is seen from a comparison of Figure 7 with Figures 4 through 6 that an isoclinic appears as a dark region.

It should be mentioned that it was found virtually impossible to completely eliminate isochromatic fringe patterns when isoclinic patterns were being photographed, whereas the reverse was possible. Note that isoclinic patterns were taken by removing the quarter-wave plates from the optical system (see Fig. 1). However, the presence of the isochromatic patterns was not a severe problem insofar as analyzing the isoclinic patterns was concerned, because separate photographs of isochromatic fringe patterns helped isolate the isoclinic patterns. Also, when color pictures were taken using a white light source, isoclinic patterns always appeared as dark regions, while isochromatic fringe patterns were never dark. Thus, the use of color photographs also helped to isolate the isoclinic patterns. We shall describe below how isoclinic



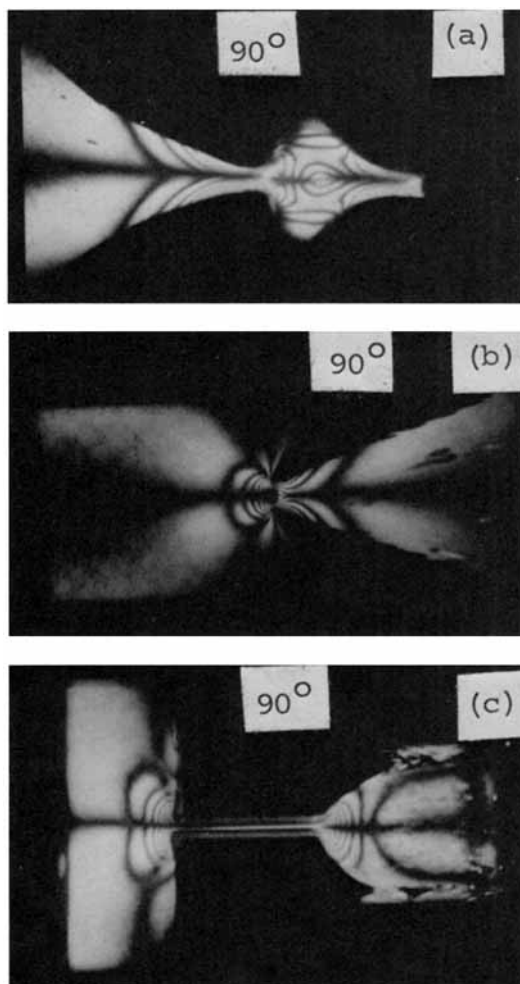


Fig. 7. Representative isoclinics in dies 2a, 2b, and 2c for polystyrene at 200°C.

patterns can be used, together with isochromatic fringe patterns, in order to obtain quantitative information of stresses in a given flow field.

Finally, in Figures 8 through 10, we present representative pictures of isochromatic fringe patterns for die 3a, die 3b, and die 3c, respectively. It will be recalled that these flow geometries were chosen for the purpose of simulating the stress distributions of polymer melts encountered in injection molding operations with "metal inserts" in the mold cavity.

One of the important technical problems associated with molding thermoplastics in a mold having a metal insert is to have a uniform stress distribution across the surface of the metal insert. A poor distribution of stresses can often lead to environmental cracking later. Of course, there are many variables which are important to the success of the injection molding operation. In the present study, however, we were interested primarily in understanding the stress distributions at various locations between the die surface and the metal insert. Note, however, that our experiments were carried out with a constant flow rate of thermoplastics under isothermal conditions.

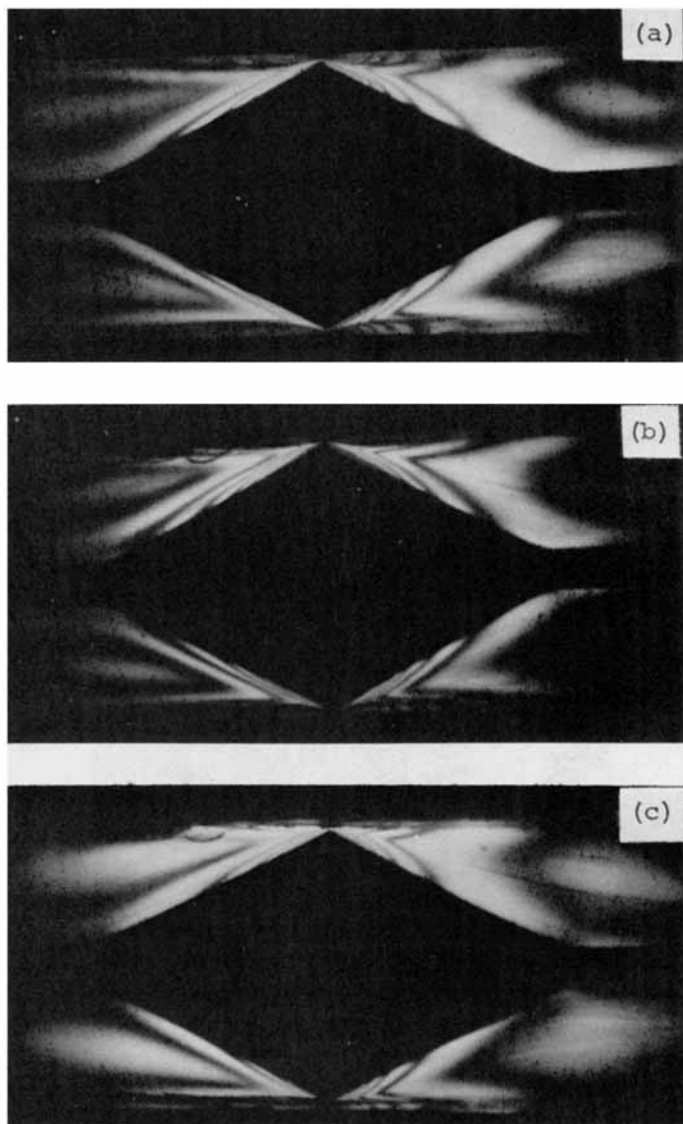


Fig. 8. Isochromatic fringe patterns in die 3a for high-density polyethylene: (a)  $Q = 49.23$  cc/min,  $T = 240^\circ\text{C}$ ; (b)  $Q = 30.11$  cc/min,  $T = 200^\circ\text{C}$ ; (c)  $Q = 8.21$  cc/min,  $T = 180^\circ\text{C}$ .

Figure 8 gives isochromatic fringe patterns of high-density polyethylene in die 3a at different melt temperatures. It is seen that the highest stress concentration occurs at the sharp edges (upper and lower), as expected, and that the same level of stresses may be achieved at a low flow rate, by lowering the melt temperature. It was observed that the stress birefringence pattern is very sensitive to temperature. Figure 9 gives isochromatic fringe patterns of polystyrene at  $200^\circ\text{C}$  in die 3b for different flow rates, and Figure 10, the same for die 3c. Note that the rheological implication of the isochromatic fringe patterns in Figures 8 through 10 is the same as that described above in connection with Figures 4 through 6. We have also taken photographs of iso-

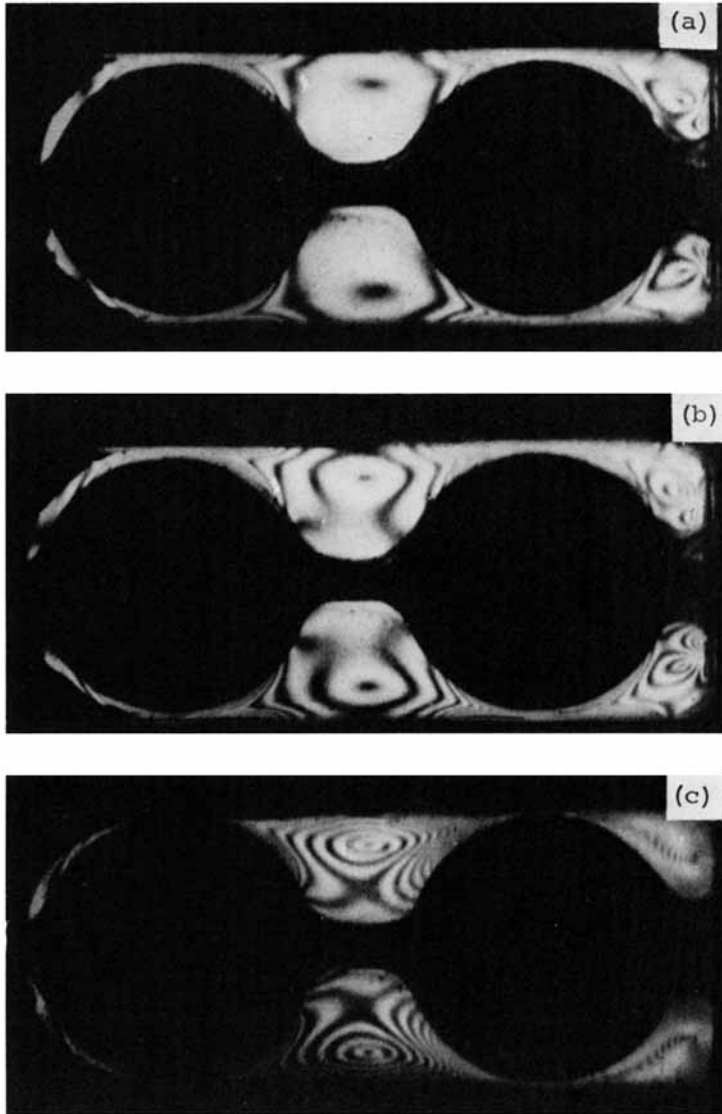


Fig. 9. Isochromatic fringe patterns in die 3b for polystyrene at 200°C: (a)  $Q = 7.91$  cc/min; (b)  $Q = 13.21$  cc/min; (c)  $Q = 15.09$  cc/min.

clinic patterns for each isochromatic fringe pattern given in Figures 8 through 10. However, space limitations does not permit us to present those isoclinic pictures in this paper.

#### Procedures of Stress Birefringence Data Analysis

In order to obtain quantitative information from the isochromatic fringe patterns and isoclinics, one has to label each of the isochromatic fringes in correct numerical order. For this, one has to know how the fringes develop. Sometimes it is very difficult to know from static pictures alone how the frin-

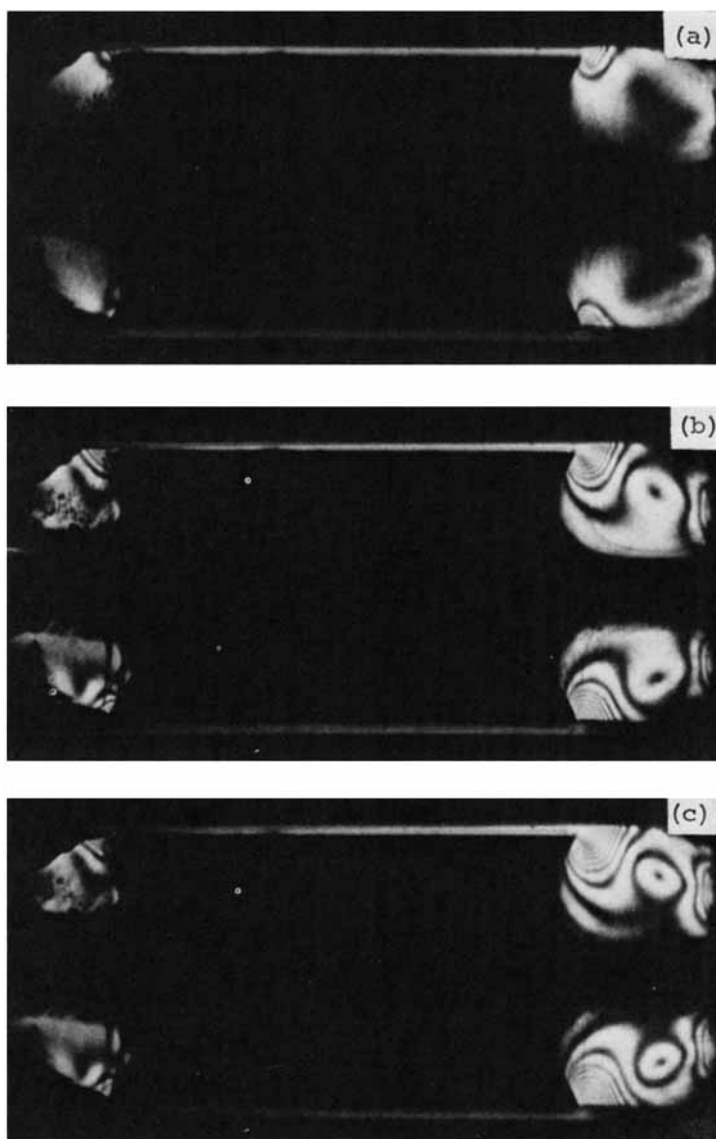


Fig. 10. Isochromatic fringe patterns in die 3c for polystyrene at 200°C: (a)  $Q = 10.21$  cc/min; (b)  $Q = 15.02$  cc/min; (c)  $Q = 21.02$  cc/min.

ges actually develop. For instance, it is not clear in Figure 4 whereabouts the fringes first start to develop. In such instances, taking motion pictures is of great help in following how stresses develop when flow starts from rest. In the present study, motion pictures were taken of the stress buildup phenomenon for all six dies tested.

Having carefully studied the motion pictures taken, we were able to label each of the isochromatic fringes in correct numerical order. Representative results are given in Figures 11 to 13 for flow in dies 2a, 2b, and 2c, respectively. The lines in these figures are drawn through the center of the black and white bands (isochromatics) in the pictures of isochromatic fringe patterns,

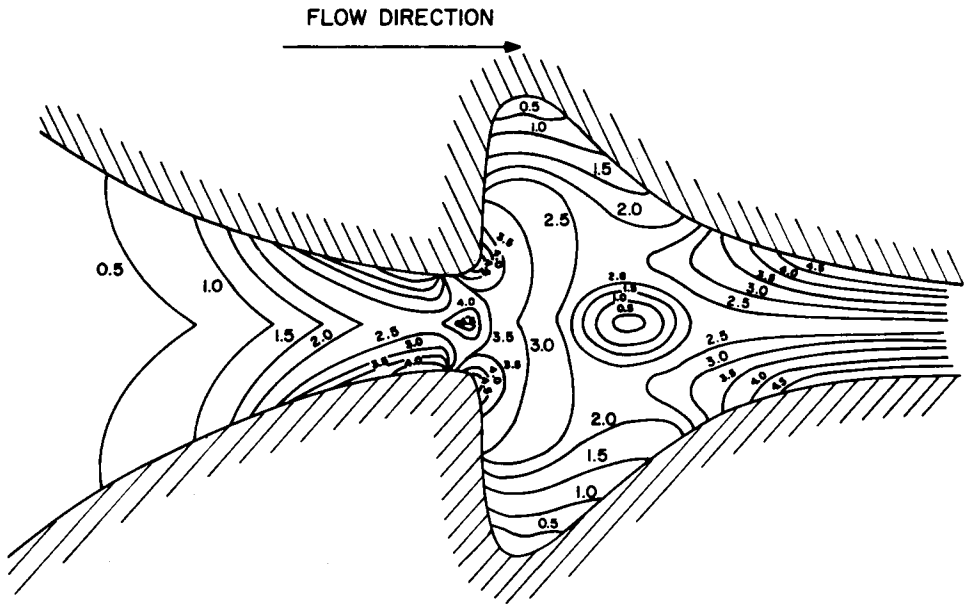


Fig. 11. Isochromatic fringe orders in die 2a for polystyrene at 200°C ( $Q = 5.15$  cc/min).

and the numbers given on each line denote the order  $N$  of the fringe, see eq. (3). It should be noted that the lines having higher orders of fringe have greater stresses than those having lower orders of fringe. Note that, in all cases, stresses are distributed symmetrically about the centerline.

A few interesting observations may be made in Figures 11 to 13. First, it is seen that as the fluid flows from the left to the right, the order of fringes increases in the left-half die, indicating that stresses build up in the fluid. This in turn indicates that the flow is in an accelerative flow field (i.e., in the converging flow field). Second, it is seen in Figures 11 to 13 that the order of fringes decreases as the fluid flows from the left to the right in the right half of the die. The decrease in the order of fringes indicates that the flow is in a decelerative flow field (i.e., in the diverging flow field). Of course, the manner in which stresses build up and relax depends very much on the geometry of a die, as amply demonstrated in Figures 4 to 6.

We shall now outline very briefly the procedures used to obtain point values of stresses in the flow field concerned. First, in order to accurately read off the fringe order and isoclinic angle at various positions in the flow field, a rectangular grid is constructed on pictures of isochromatic and isoclinic fringe patterns. Because of the symmetry involved in this type of analysis, only one half of the flow region about the centerline in the direction of flow is to be considered. The fringe order and the isoclinic angle are determined at each grid point. In order to facilitate the reading of the isoclinic angle, it is convenient to combine the isoclinic patterns into one figure representing the family of isoclinics between  $0^\circ$  and  $90^\circ$  in increments of  $10^\circ$ . A representative example is shown in Figure 14. This was obtained by tracing the photographic patterns onto one master drawing. It should be noted that as the isoclinic lines on the photographs appear as broad, black lines (see Fig. 7), a line representing the fringe is to be drawn through the center of the pat-

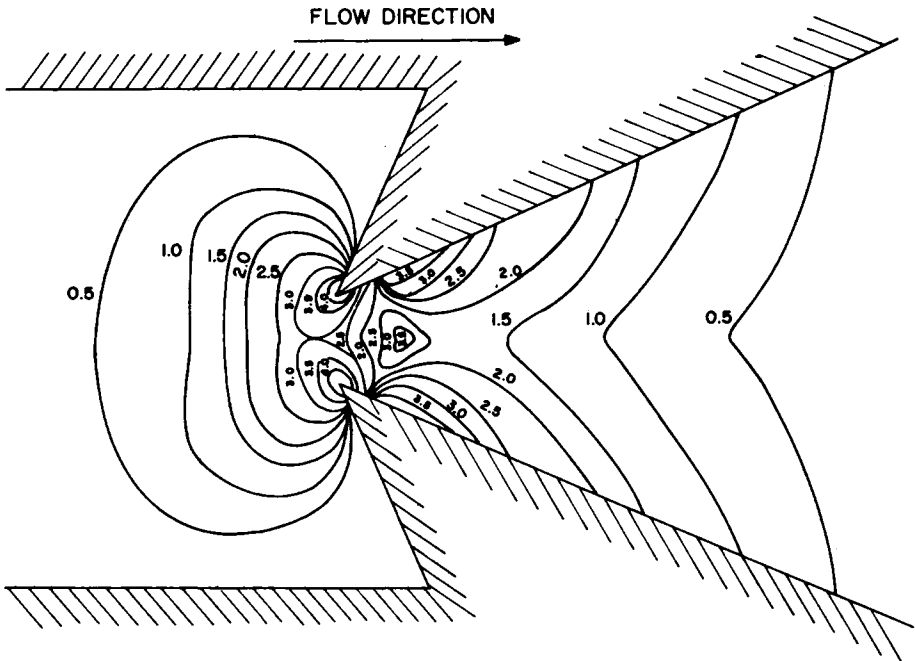


Fig. 12. Isochromatic fringe orders in die 2b for polystyrene at 200°C ( $Q = 7.21$  cc/min).

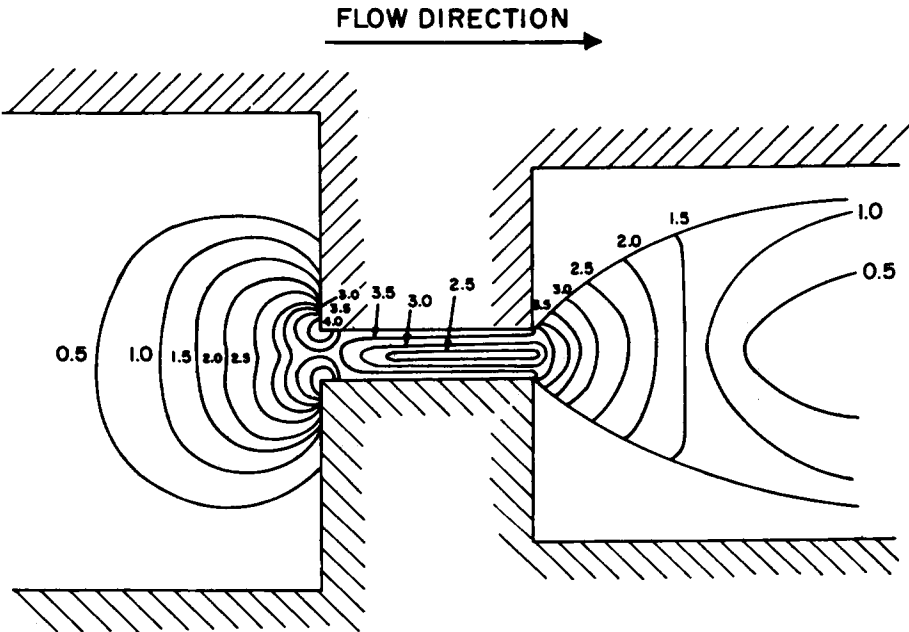


Fig. 13. Isochromatic fringe orders in die 2c for polystyrene at 200°C ( $Q = 6.54$  cc/min).

tern. As one may surmise, the narrower the isoclinic lines are, the more accurate will be the reading of the isoclinic angle.

Now, the data-reduction procedure is to draw horizontal and vertical lines on both the isochromatic pattern photograph and on the combined isoclinic

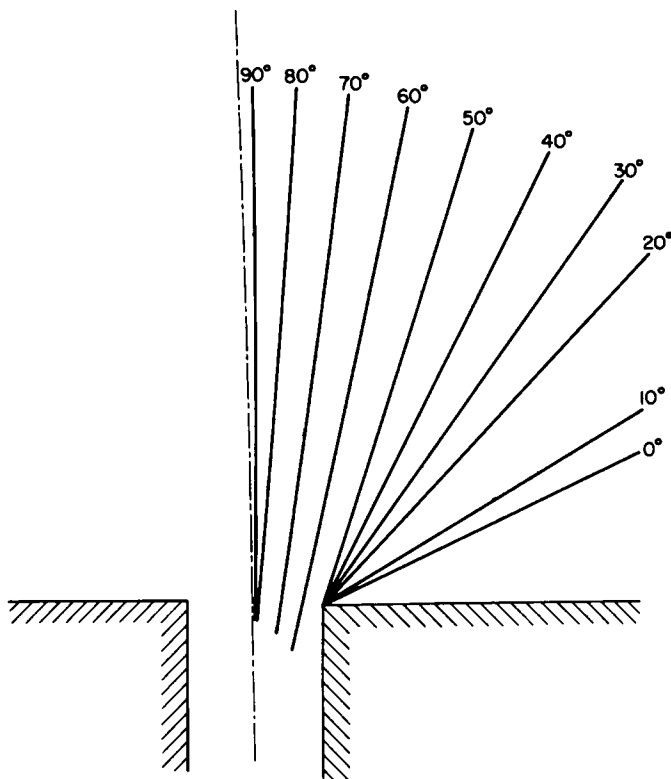


Fig. 14. A family of isoclinics between  $0^\circ$  and  $90^\circ$  in die 2c for polystyrene at  $200^\circ\text{C}$ .

drawing. The fringe order and its associated horizontal position is then recorded along each of the horizontal lines. In a similar manner, the isoclinic angles and their respective horizontal positions are recorded. It is important to note that the family of isochromatic fringes recorded from using a *light* field circular polariscope represents a half-order of interference (see Figs. 11 to 13). In order to obtain the fringe order and isoclinic angle at the specific grid points, it is necessary to interpolate between the above recorded positions. It is possible then to obtain the fringe order and the isoclinic angle at specific coordinate positions. It must be remembered that distances read from the photographs are to be converted to actual distances by direct proportion, knowing the magnification used.

#### Determination of Stress Distribution

Having recorded both isochromatic and isoclinic fringe patterns, we can now quantitatively determine the distributions of stresses in the flow field concerned, with the assumption that the melts investigated follow the stress optical laws<sup>12-14</sup>:

$$\Delta n = C\Delta\sigma \quad (1)$$

$$\theta_{\text{opt}} = \theta_{\text{stress}} = \theta \quad (2)$$

in which  $\Delta n$  is the magnitude of birefringence defined as

$$\Delta n = N\lambda/d. \quad (3)$$

Equation (1) states that the relative retardation  $N$  (or fringe order) is proportional to the difference in two principal stresses  $\Delta\sigma$ , and eq. (2) states that the orientation of the optical axes is identical with that of the principal stress axes. The proportionality constant  $C$  appearing in eq. (1) is called the stress optical coefficient, which is a characteristic of the fluid under consideration. Note in eq. (3) that  $\lambda$  is the wavelength of the light entering an optically anisotropic medium (i.e., in the present study, the polymer melt in flow) and that  $d$  is the thickness of the medium that the light must pass through. It should be noted that, in the past, eqs. (1) and (2) were tested with success for polymer solutions<sup>15-18</sup> and for polymer melts.<sup>5,19,20</sup>

Since eqs. (1) and (2) are referred to the principal coordinates, the stresses must be transformed from the principal coordinates to the Cartesian coordinates by rotation. This transformation yields shear stress  $\tau_{xy}$  and difference in normal stresses  $\tau_{xx} - \tau_{yy}$ , in terms of principal stress  $\Delta\sigma$ , as follows<sup>21,22</sup>:

$$\tau_{xy} = \frac{\Delta\sigma}{2} \sin 2\theta_{\text{stress}} \quad (4)$$

$$\tau_{xx} - \tau_{yy} = \Delta\sigma \cos 2\theta_{\text{stress}}. \quad (5)$$

Using eqs. (1) and (2), eqs. (4) and (5) may be rewritten as

$$\tau_{xy} = \frac{\lambda N}{2Cd} \sin 2\theta \quad (6)$$

$$\tau_{xx} - \tau_{yy} = \frac{\lambda N}{Cd} \cos 2\theta \quad (7)$$

where  $\theta$  is the isoclinic angle and  $N$  is the order of fringe to be read from the isochromatic fringe patterns.

It is then seen from eqs. (6) and (7) that in order to calculate  $\tau_{xy}$  and  $\tau_{xx} - \tau_{yy}$ , the stress optical coefficient  $C$  must be known beforehand for the fluid being investigated.

Figures 15 through 17 give distributions of shear stress for polystyrene melts at 200°C in die 2a, die 2b, and die 2c, respectively. Note that in constructing the stress distributions in the flow fields concerned, use is made of the numerical value of the stress optical coefficient together with eq. (6) given above. Some interesting observations may be made in Figures 15 through 17.

It is seen in Figure 15 that, in the left half of the die, stresses are seen in the nature of converging flow, whereas in the right half of the die, stresses relax somewhat at and near the centerline, and then build up again as the melt approaches the die exit.

It is seen in Figure 16 that in the left half of the die, stresses form a loop, showing clear evidence of converging flow, whereas in the right half of the die, stresses relax in a pattern which looks very similar to the stress distributions in the opposite direction of the left half of Figure 15.

It is seen in Figure 17 that the stress distributions in the left half of the die look very similar to those in the left half of the die in Figure 16. However the stress distributions in the right half of the dies in these figures are somewhat



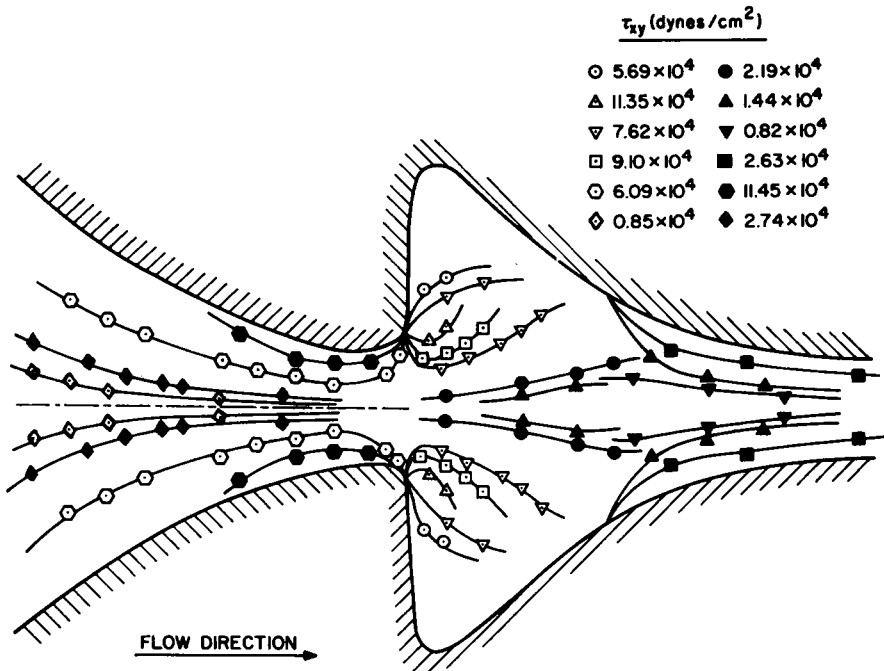


Fig. 15. Shear stress distributions in die 2a for polystyrene at 200°C ( $Q = 5.15$  cc/min).

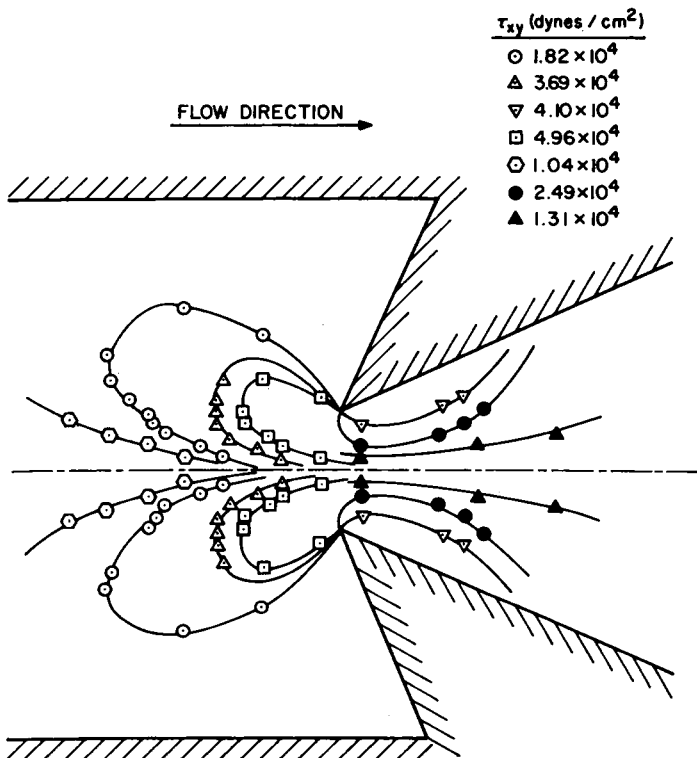


Fig. 16. Shear stress distributions in die 2b for polystyrene at 200°C ( $Q = 7.21$  cc/min).

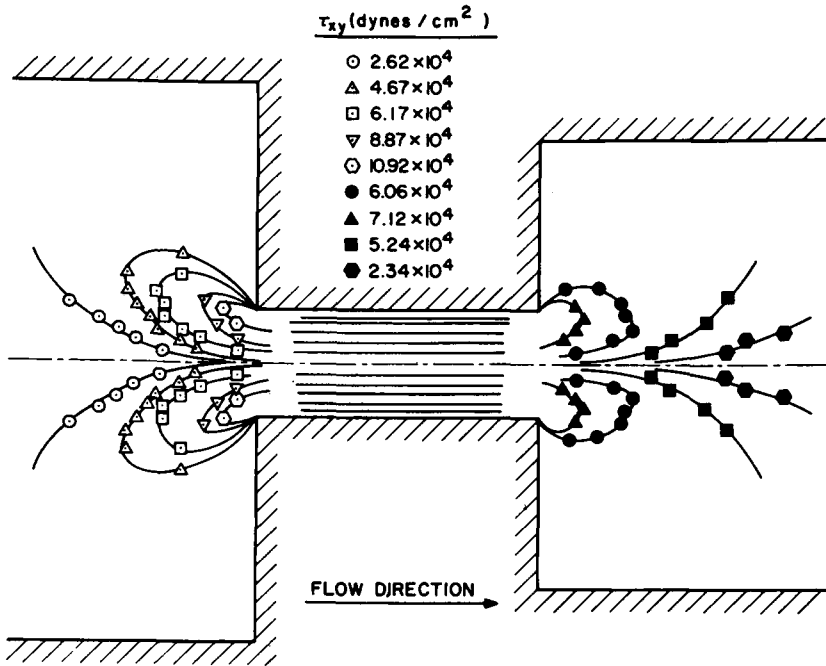


Fig. 17. Shear stress distributions in die 2c for polystyrene at 200°C ( $Q = 6.54$  cc/min).

different. The difference is attributed to the geometry of the die. It is interesting to note in Figure 17 that stress distributions in the right half of the die are quite similar, but in the opposite direction, to those on the left half of the die, which is as expected from the die geometry. This seems to indicate that when the geometry of a die is the same for the converging and diverging sections, information for diverging flow may be obtained from that for converging flow, and vice versa.

It is to be noted in Figure 17 that stresses in the straight section are parallel to the die wall if flow is fully developed. In the construction of Figure 17, it was not possible to quantitatively obtain the level of stresses in the straight section, because the crowding of isochromatics made it difficult for us to read off the order of fringes. Note, however, that in an earlier paper by the author,<sup>5</sup> a quantitative analysis was presented of the fully developed flow of polystyrene melts in such passages.

### CONCLUDING REMARKS

The present study demonstrates that the flow birefringence technique is a very useful tool for the study of stress distributions of rheologically complex viscoelastic polymer melts in a geometrically complex flow channel. This is very important from the practical standpoint, in particular when a rigorous theoretical analysis of the flow behavior in a given flow field is very difficult, if not totally impossible, because of the geometrical complexity of the flow channels often encountered in many polymer operations, such as in fiber spinning, injection molding, blow molding, etc.

It is shown in this paper that one can obtain quantitative information of the stress distributions of the polymer melt in the entire flow field as long as one can take photographs of isochromatic and isoclinic fringe patterns in the field and one knows the stress optical coefficient of the material being investigated. Note that one can easily determine the stress optical coefficient, by constructing a thin slit die and taking wall normal stress measurements as described in a paper by Han and Drexler.<sup>5</sup>

There are, however, some limitations of the experimental technique described above: first, the flow channel should have flat surfaces through which a light beam passes; second, as flow rate is increased, the number of fringes also increases, making the identification of different fringe orders very difficult; third, there is no proven theoretical justification for the use of the stress-optical laws for nonviscometric flows.

It should be noted further that in computing the point values of stress given in Figures 15 to 17, gradients in the direction of viewing are assumed to be negligible. This assumption is valid only when the die dimension in the viewing direction is large compared to its width (i.e., narrow slit approximation). Therefore, one cannot assess the validity of this assumption from the information presented. This, however, is of relatively minor importance, since it is the stress distribution, rather than the absolute value, which is of most interest.

Despite the limitations mentioned above, the author feels that the flow birefringence technique is a very useful tool to study the polymer melt flow in geometrically complex dies. Such study will help one to determine the optimum geometrical configuration of complex extrusion dies and molds.

### References

1. E. B. Adams, J. C. Whithead, and D. C. Bogue, *A.I.Ch.E. J.*, **11**, 1026 (1965).
2. K. Funatsu and Y. Mori, *Kobunshi Kagaku*, **25**, 337 (1968).
3. R. L. Boles, H. L. Davis, and D. C. Bogue, *Polym. Eng. Sci.*, **10**, 24 (1970).
4. T. Arai and H. Asano, *Kobunshi Kagaku*, **29**, 510 (1972); *ibid.*, **29**, 743 (1972).
5. C. D. Han and L. H. Drexler, *J. Appl. Polym. Sci.*, **17**, 2329, 2369 (1973).
6. C. D. Han and L. H. Drexler, *Trans. Soc. Rheol.*, **17**, 659 (1973).
7. E. B. Bagley and A. M. Birks, *J. Appl. Phys.*, **31**, 556 (1960).
8. T. F. Ballenger and J. L. White, *J. Appl. Polym. Sci.*, **15**, 1949 (1971).
9. E. A. Uebler, Ph.D. Thesis, University of Delaware, Newark, Delaware, 1966.
10. L. H. Drexler and C. D. Han, *J. Appl. Polym. Sci.*, **17**, 2355 (1973).
11. C. D. Han, *A.I.Ch.E. J.*, **19**, 649 (1973).
12. A. S. Lodge, *Trans. Faraday Soc.*, **52**, 127 (1956).
13. W. Philippoff, *J. Appl. Phys.*, **27**, 984 (1956).
14. J. L. S. Wales and H. Janeschitz-Kriegl, *J. Polym. Sci. A-2*, **5**, 781 (1967).
15. W. Philippoff, *Trans. Soc. Rheol.*, **1**, 95 (1957).
16. W. Philippoff, *Trans. Soc. Rheol.*, **5**, 163 (1961).
17. J. L. den Otters, Doctoral Dissertation, University of Leiden, 1967.
18. H. Janeschitz-Kriegl, *Advan. Polym. Sci.*, **6**, 170 (1969).
19. F. D. Dexter, J. C. Miller, and W. Philippoff, *Trans. Soc. Rheol.*, **5**, 193 (1961).
20. J. L. S. Wales, *Rheol. Acta*, **8**, 38 (1969).
21. M. M. Frocht, *Photoelasticity*, Vol. 1, Wiley, New York, 1941.
22. A. W. Hendry, *Photoelastic Analysis*, Pergamon Press, New York, 1966.